

## A Solid-state NMR Study of the Kinetics of the Activity of an Antimicrobial Peptide, PG-1 on Lipid Membranes

Chul Kim\* and Sungsool Wi†,\*

*Department of Chemistry, Hannam University, Daejeon 305-811, Korea. \*E-mail: chulkim@hnu.kr*

*†Department of Chemistry, Virginia Tech, Blacksburg, VA 24061, USA. \*E-mail: sungsool@vt.edu*

*Received September 23, 2011, Accepted November 28, 2011*

The activity of an antimicrobial peptide, protegrin-1 (PG-1), on lipid membranes was investigated using solid-state NMR and a new sampling method that employed mechanically aligned bilayers between thin glass plates. At 95% hydration and full hydration, the peptide respectively disrupted 25% and 86% of the aligned 1-palmitoyl-2-oleoyl-*sn*-glycero-3-phosphatidylcholine (POPC) bilayers at a P/L (peptide-to-lipid) ratio of 1/20 under the new experimental conditions. The kinetics of the POPC bilayers disruption appeared to be diffusion-controlled. The presence of cholesterol at 95% hydration and full hydration reduced the peptide disruption of the aligned POPC bilayers to less than 10% and 35%, respectively. A comparison of the equilibrium states of heterogeneously and homogeneously mixed peptides and lipids demonstrated the importance of peptide binding to the biomembrane for whole membrane disruption.

**Key Words :** Antimicrobial peptide, Lipid bilayer, Hydration, Cholesterol, Solid-state NMR

### Introduction

Small antimicrobial peptides (AMPs) show bactericidal or fungicidal activity. Studies of their reaction mechanisms with biomembranes have been carried out to elucidate the nature of their activity.<sup>1-4</sup> These peptides can usually react with cell membranes directly through elementary chemical interactions without requiring other receptor proteins in the membrane.<sup>5</sup> The AMP reactivity depends on the strength of its elementary chemical interactions with lipids,<sup>5</sup> which comprise electrostatic interactions between the positively charged peptide and the negatively charged membrane surface and hydrophobic interactions between hydrophobic side chains of the peptide and acyl chains of the lipid molecules. Many other interactions also affect AMPs reactivity with biomembranes: interactions among the lipid molecules, peptide-peptide interactions, and interactions of peptide and lipid molecules with environmental molecules, e.g. water molecules surrounding the peptide-lipid mixtures.<sup>6</sup> These interactions are generally related to the molecular structure and the chemical properties of the peptide and the lipid:  $\alpha$ -helical or  $\beta$ -sheet structure of the peptide,<sup>7</sup> the charge densities of the peptide and the head groups of the lipid,<sup>8</sup> the lipid chain length,<sup>9,10</sup> and the constituents of the biomembrane.<sup>8</sup> The interactions also depend on the microscopic structure of the membrane surface. The membrane system can be represented as a mosaic of liquid-disordered ( $l_d$ ) and liquid-ordered ( $l_o$ ) domains, with the liquid-disordered domains consisting of only lipids and the liquid-ordered domain consisting of lipids, cholesterol, proteins, *etc.* Antimicrobial peptides have been shown to act more effectively on liquid-disordered domains.<sup>11</sup> These factors have been studied using lipid vesicles in solution<sup>12,13</sup> and by using fluorescence,<sup>13,14</sup> CD,<sup>14,15</sup> NMR,<sup>16</sup> *etc.*<sup>16,17</sup> Kinetic

studies of AMP activity have been also performed in various solution phases.<sup>12,13,18-20</sup>

In addition to liquid-state NMR, solid-state NMR (SSNMR) has also been used to study the reaction mechanism of AMPs by measuring the geometrical distribution of the disrupted lipid molecules and the binding orientation of the peptide molecules in the lipid membranes.<sup>9,21,22</sup> Solid-state NMR spectra of mechanically aligned bilayers (multi-bilayers) can help elucidate the mechanism of AMPs' activity. A membrane thinning model,<sup>23-25</sup> a carpet model,<sup>26-28</sup> and a pore model<sup>1,12,29-31</sup> of membrane bilayers have been suggested from interpreting SSNMR data. However, SSNMR has been generally used to investigate the equilibrium states of peptide-lipid mixtures. Mechanically aligned bilayers, generally used in solid-state NMR studies of membrane systems, are prepared by the homogeneous mixing of peptides and lipids in an appropriate organic solvent, drying the organic solvent, and then hydrating the peptide-lipid mixture with water. Such samples do not allow the observation of intermediate states during membrane disruption. It is questionable that how well such systems represent the biological reaction that occur in cells and whether their final state is comparable to that which occurs biologically. Membrane degradation by the attack of an antimicrobial peptide occurs through the intermediate state.

This work reports a new experimental method using heterogeneously mixed samples for the kinetic study of the reactions of AMPs. The method is a modification of the sampling method used for mechanically aligned multi-bilayers to allow closer resemblance of biological situations. Lipid bilayers and peptides were prepared on separate glass plates without mixing. They were then allowed to make contact by stacking the glass plates. <sup>31</sup>P SSNMR spectra were recorded as their reaction proceeded. The tested prote-

grin-1 (PG-1) antimicrobial peptide is a cysteine-rich, 18-residue  $\beta$ -sheet peptide isolated from porcine leukocytes. It has antimicrobial activity against a broad range of microorganisms.<sup>32</sup>

Reaction rate constants were measured using variously hydrated lipid multi-bilayers to observe the effects of the water contents on the activity of PG-1 against the lipid multi-bilayers. Cholesterol was also shown to affect strongly PG-1's activity towards the lipid multi-bilayers. Other advantages of heterogeneously mixed sampling over homogeneously mixed sampling were demonstrated through a comparison of SSNMR spectra.

### Materials and Methods

**Materials.** 1-Palmitoyl-2-oleoyl-*sn*-glycero-3-phosphocholine (POPC) was purchased from the Avanti Polar Lipids (Alabaster, AL) and used without further purification. The main phase transition temperature of POPC is  $-2^{\circ}\text{C}$ . Protegrin-1 was purchased from GL Biochem (Shanghai, China). Trifluoroethanol (TFE), chloroform and sodium phosphate dibasic were purchased from the Aldrich Chemicals (Milwaukee, WI). Thin glass plates with about 80  $\mu\text{m}$  in thickness and 5 mm  $\times$  10 mm in rectangular square were purchased from the Marienfeld Laboratory Glassware (Bad Mergentheim, Germany).

**Sample Preparation.** Membranes were oriented on the glass plates by an elsewhere described procedure.<sup>8</sup> 4.8 mg POPC lipids was dissolved in TFE/chloroform (2:1), deposited on 10 glass plates at a surface concentration of  $\sim 0.0096\text{ mg/mm}^2$ , air-dried for 2-3 hours and then vacuum-dried overnight to remove any residual organic solvent. After drying, water was directly added to each glass plate using a microsyringe. The plates were then stored for 2 days at room temperature and 95% relative humidity. The relative humidity was maintained using saturated sodium phosphate dibasic solution.<sup>33,34</sup> Membranes with cholesterol were prepared from equal mixtures of POPC and cholesterol. 0.68 mg PG-1 (MW = 2154 Da) was also dissolved in TFE/chloroform (2:1), deposited on 10 glass plates and then treated similarly to the plates with lipids. The plates containing peptide and lipid were then stacked, wrapped in Parafilm, and sealed in polyethylene bag to prevent dehydration during the NMR measurements. The peptide to lipid (P/L) ratio was 1/20. The stacked glass plates were placed in a solid-state NMR probe with the glass plates normal parallel to the  $B_0$  field.  $^{31}\text{P}$  SSNMR spectra of samples stored at 95% relative humidity were recorded until they showed no further changes, indicating that the mixture of peptides and lipids had reached equilibrium. The samples were then fully hydrated by adding water to the sides of the stacked glass plates and  $^{31}\text{P}$  SSNMR spectra were rerecorded.

**Solid-state NMR.**  $^{31}\text{P}$  NMR spectra were recorded on a Bruker MSI-300 spectrometer at  $25^{\circ}\text{C}$  with a resonance frequency of 121.49 MHz.  $^{31}\text{P}$  chemical shifts were referenced to 85%  $\text{H}_3\text{PO}_4$  at 0 ppm. A typical  $^{31}\text{P}$   $90^{\circ}$  pulse length was 5  $\mu\text{s}$ . Spectra were acquired under  $^1\text{H}$  decoupling

of continuous wave (CW) with a recycle delay of 2 s. The rf field strength for  $^1\text{H}$  decoupling was 45 kHz. The spectral width for  $^{31}\text{P}$  SSNMR was 17.86 kHz. Spectra were typically averaged over 2000 scans taken over 20 minutes. When equilibrium was reached, the last spectra were recorded for 1-2 hours to obtain more accurate line shape.

### Results and Discussion

**Disruption of Lipid Bilayers by Antimicrobial Peptides in Heterogeneously Mixed Samples.** The lipid phase changed upon exposure to the peptide molecules (Fig. 1), with the alignment of the first lipid bilayer being the first to decay.<sup>35,36</sup> After the first lipid bilayer was disrupted by the peptides, the peptides could then pass through to attack and disrupt the second and subsequent lipid bilayers. The critical concentration of the peptide is the least P/L ratio at which a well-aligned lipid bilayer is disrupted. While the degradation process proceeded, the amount of peptides-lipid aggregates increased and the concentration of pure peptides decreased. Lipid bilayer disruption stopped when the peptide on the lipid membrane surface could not reach the critical concentration. Therefore measurement of the number of disrupted bilayers can be used to calculate the critical concentration. The disruption mechanism may include several sequential steps: separation (solvation) of the peptides from their initial aggregations on the glass plate, binding of the peptides to the lipid bilayer surface, disruption of the lipid bilayer, and diffusion of residual free peptides to the next bilayer. The total process, however, can be regarded as being governed by two reaction rates: the formation of peptide-lipid aggregates and the transportation of free peptides from the surface of the top glass plate to each lipid bilayer.

Though the rate of formation of peptide-lipid aggregates, i.e. the disruption of the lipid bilayers by the peptides, may depend on the strength of the peptide-lipid interactions and the membrane rigidity, molecular dynamics studies have shown that the lipid-peptide mixture reaches equilibrium after tens of nanoseconds.<sup>37,38</sup> Therefore, peptide-lipid aggregate formation can be considered to be very fast if peptide is present at the critical concentration and the overall rate is governed by the transportation time of the peptide from the

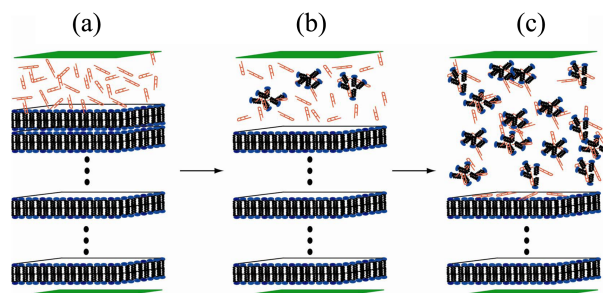


**Figure 1.** The reaction procedure. (a) Initial, (b) intermediate, and (c) final stages after placing a peptide-containing glass plate on a lipid-containing glass plate. Blue and black rods represent the lipids, red the antimicrobial peptides, and green the two glass plates.

top to the membrane surface. More rigid lipid membranes will require more peptide molecules on their surfaces to degrade them, decreasing the formation rate of peptide-lipid aggregates. The membrane rigidity is generally dependent on its level of hydration, its surface charge density, and the presence of other chemicals such as cholesterol.

The diffusion rate of free peptides from the surface of the top glass plates to each bilayer depends on the viscosity of the bulk phase. This depends on the concentration and the size of the peptide-lipid aggregates, which are affected by the hydration level. The sampling method reported here could not give detailed descriptions of the disruption process but it did generate important information about the reaction of AMPs with biomembranes by simplifying the reaction process.

**Disruption of POPC Bilayers by PG-1.** The two glass plates containing peptides and POPC were initially stacked when hydrated at 95% relative humidity. Upon reaching equilibrium, water drops were applied to the sides of the stacked glass plates to fully hydrate the lipid-peptide mixture. The series of  $^{31}\text{P}$  SSNMR spectra (Fig. 2) shows that

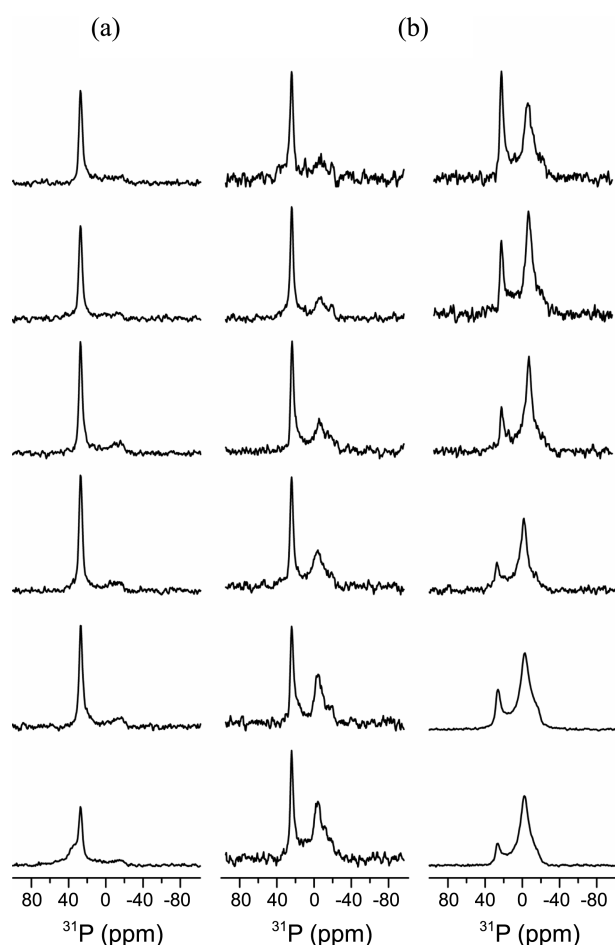


**Figure 2.**  $^{31}\text{P}$  SSNMR spectral changes of POPC multi-bilayers by PG-1. (a) 20, 40, 70 minutes and 9, 19, 46 hours (from top to bottom) after stacking the glass plates at when hydrated at 95% humidity. (b) (left) 10, 15, 30, 50, 100, 130 minutes and (right) 3.5, 8, 20, 44.5, 51, 177 hours (from top to bottom) after fully hydrating the sample by adding water.

lipid molecules in the well-aligned bilayers gave a sharp peak at 35 ppm, whereas in the peptide-lipid aggregates the lipid molecules gave a broad peak in the range of  $-15$  ppm to 31 ppm because of the broad angular distribution of their molecular axes. The relative amounts of lipid molecules in the well-aligned bilayers and in the peptide-lipid aggregates could be calculated by integrating the two peaks of the  $^{31}\text{P}$  SSNMR spectra.

In the POPC bilayers hydrated at 95% relative humidity, 25% of the aligned bilayers were disrupted by PG-1 peptide. At equilibrium, the peptide-lipid aggregates had a P/L ratio of 1/5, which was calculated from the amount of disrupted lipids of which the value was determined from the integral value of the peak in the range of  $-15$  to 31 ppm and the total amount of peptides in the mixture. All the peptide molecules were assumed to have formed peptide-lipid aggregates when equilibrium had been reached: unlike in solution, all the free peptides could react with each bilayer sequentially. Thousands of bilayers were stacked and hundreds were disrupted.  $6.33 \times 10^{-6}$  moles of POPC was deposited on 10 glass plates. If the normal area of each POPC molecule is  $68.3 \text{ \AA}^2$ ,<sup>39</sup> the number of bilayers will be *ca.* 2610 between the two glass plates, 653 bilayers of which (25%) were disrupted. Therefore the amount of peptide needed to disrupt a single bilayer was negligibly small compared with total amount of peptide involved in the disruption of hundreds of bilayers.

The  $^{31}\text{P}$  SSNMR spectra of the disrupted lipids over the course of the reaction fitted those of a mixture of an aligned bilayer and a random powder. The random powder patterns suggest that the disrupted peptide-lipid aggregates were not mobile, likely due to their large size at high aqueous lipid concentrations. The disruption of 25% of the lipid bilayers occurred within 1 hour of the reaction starting; no subsequent disruption was observed.

However when the bilayers were fully hydrated, degradation of the aligned bilayers resumed, with 86% of them being eventually disrupted. Disruption produced more than two phases: one highly mobile phase which gave an isotropic  $^{31}\text{P}$  SSNMR peak at 0 ppm, and others that moved slowly, which gave typical powder patterns in the spectra. The P/L ratio of the peptide-lipid aggregates was calculated to be 1/17, similar to the critical concentration of antimicrobial peptides in biological membrane systems.<sup>33,40</sup> The P/L ratios demonstrate the strong effect that hydration had on the disruption of the lipid membranes. The spectra were well fitted as the sum of signals from the aligned bilayers and the random powder of peptide-lipid aggregates with isotropic random tumbling motion at various tumbling rates (Fig. S1).

The low disruption of the lipid bilayers at 95% hydration was due to their increased rigidity. The low water content between the bilayers allowed them to be close to each other, enabling strong electrostatic interactions between their head groups that increased rigidity. The lipid membranes studied here could be considered as multi-bilayers, rather than isolated bilayers, that were more difficult to disrupt than isolated bilayers. When fully hydrated, with a water content

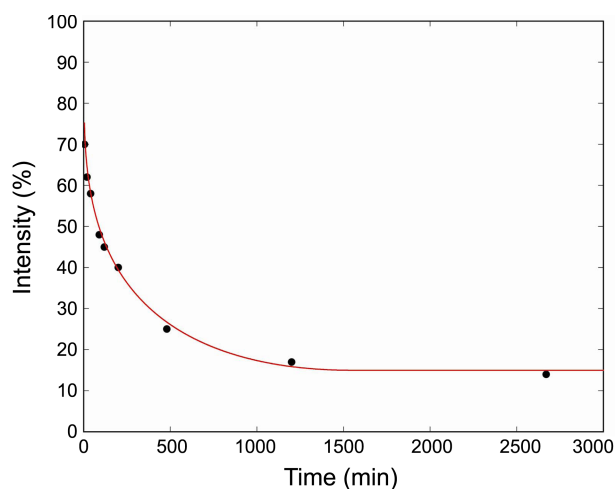


**Figure 3.** Integrated intensity changes of the peak at 28 ppm in the  $^{31}\text{P}$  SSNMR spectra in Figure 2. Dots are experimental data points and the solid line is the decay curve fitted with the diffusion equation in the text.

between the bilayers that was similar to that of membrane surfaces of lipid vesicles in bulk solutions, the multi-bilayers could be considered as a series of free, single bilayers that were more easily disrupted by lower concentrations of antimicrobial peptides that were similar to the critical concentration observed in solution.<sup>39</sup>

The progression of lipid disruption observed at full hydration was compared with that theoretically calculated (Fig. 3). The calculation considered the reaction to be governed by peptide diffusion to the membrane surface. At  $t = 0$  all the peptides were present at the top glass plate surface, they then diffused into the bulk phase. The peptide concentration,  $c(x, t)$ , at time,  $t$ , and distance,  $x$ , from the surface of the top glass plate is given by the following well-known equation.

$$c(x, t) = \frac{c_0}{A\sqrt{\pi Dt}} \exp\left(-\frac{x^2}{4Dt}\right),$$

where  $c_0$  is a total concentration at the glass plate surface of area  $A$  and  $D$  is the diffusion coefficient.

When the simulated peptide concentration at the lipid bilayer surface reaches the cutoff of the critical concentration,  $c_{\text{off}}$ , the lipid bilayer will be disrupted. Calculation of the time at which the concentration,  $c(x, t)$  is the critical concentration at distance  $x$  can be used to generate a time curve of distance,  $x(t)$ . The thickness of each hydrated bilayer was calculated to be 11.7 nm by summing the thickness of a POPC lipid bilayer and that of the interbilayer water phase: 4 nm<sup>41</sup> and 7.7 nm, respectively. 2  $\mu\text{L}$  water was added to the POPC bilayers between the two 10 mm  $\times$  10 mm glass plates, implying a total thickness of water of 20000 nm. The thickness of the water phase between each pair of POPC bilayers was 7.7 nm because the total thickness of water was distributed among 2610 POPC lipid bilayers.

Given the distance  $x(t)$  at time  $t$ , the number of disrupted bilayers can be calculated by dividing  $x(t)$  by thickness of a

single layer (11.7 nm). From the best simulation of the experimental data a diffusion coefficient,  $D$ , of  $1.2 \times 10^{-15} \text{ m}^2/\text{s}$  was calculated using a 10 nm lamella spacing of the fully hydrated POPC bilayers rather than 11.7 nm by considering the change of the lipid bilayer thickness upon hydration and the change of water phase thickness upon insertion of water molecules into the lipid bilayers. Lipid bilayer thickness can be decreased by up to 2 nm in the case of DLPC.<sup>42</sup>

The theoretical curve simulated by the above diffusion equation fitted the experimental data well, suggesting that membrane disruption was governed by the diffusion of the peptide from the glass plate surface to the lipid bilayers. Particle diffusion in aqueous solutions depends on their hydrodynamic radius and the viscosity of the solution according to the Stokes-Einstein relation. The viscosity of the solution depends on the concentration of dissolved particles. The increasing concentration of lipid-peptide aggregates that emerged during the disruption of the lipid bilayers would be expected to increase the viscosity of the aqueous phase, decreasing the diffusion rate of peptide molecules. However, the experimental data could be fitted with a constant diffusion coefficient, implying unchanging viscosity. This was due to water being distributed evenly between the bilayers: as one bilayer was disrupted, the water it contained was added to the aqueous phase between the free peptide on the top glass plate and the undisturbed bilayers, canceling any viscosity increase from the increased presence of newly formed lipid-peptide aggregates. The concentration of the lipid-peptide aggregates, and hence the viscosity of the solution phase, remained constant and therefore the diffusion coefficient of the peptide was not altered. The rate of lipid bilayer disruption was measured and the percentage of the disrupted lipid bilayers was assessed at two hydration levels. Testing at various hydration levels would yield more detailed information about the process of bilayer disruption.

Here, the detailed structure of the peptide-lipid aggregates is not analyzed. PG-1 has been well known to make a pore in lipid bilayers prepared in the vesicle solution and the oriented bilayer phase.<sup>9</sup> In the most SSNMR studies using the oriented bilayer phase the samples were generally prepared by homogeneously mixing the peptides and the lipids at a given P/L ratio.<sup>8,43</sup> In those cases the pore formation was determined by simulating the lineshapes of the experimental  $^{31}\text{P}$  and  $^2\text{H}$  SSNMR spectra. However, as Mei Hong *et al.* indicated in their paper,<sup>9</sup> increasing the PG-1 concentration increases the number of such toroidal pores, eventually will destroy the alignment of the lipid bilayer and the pore structure. In our sample the P/L ratio of the most bilayers disrupted by PG-1 will be hugely high and it is reasonable that there is no pore structure during the bilayer disruption process.

**Disruption of POPC/Cholesterol Bilayers by PG-1.** POPC/cholesterol bilayers were similarly analyzed. A lipid-cholesterol ratio of 1:1 resulted in less than 10% of the aligned bilayers being disrupted by PG-1 when hydrated at

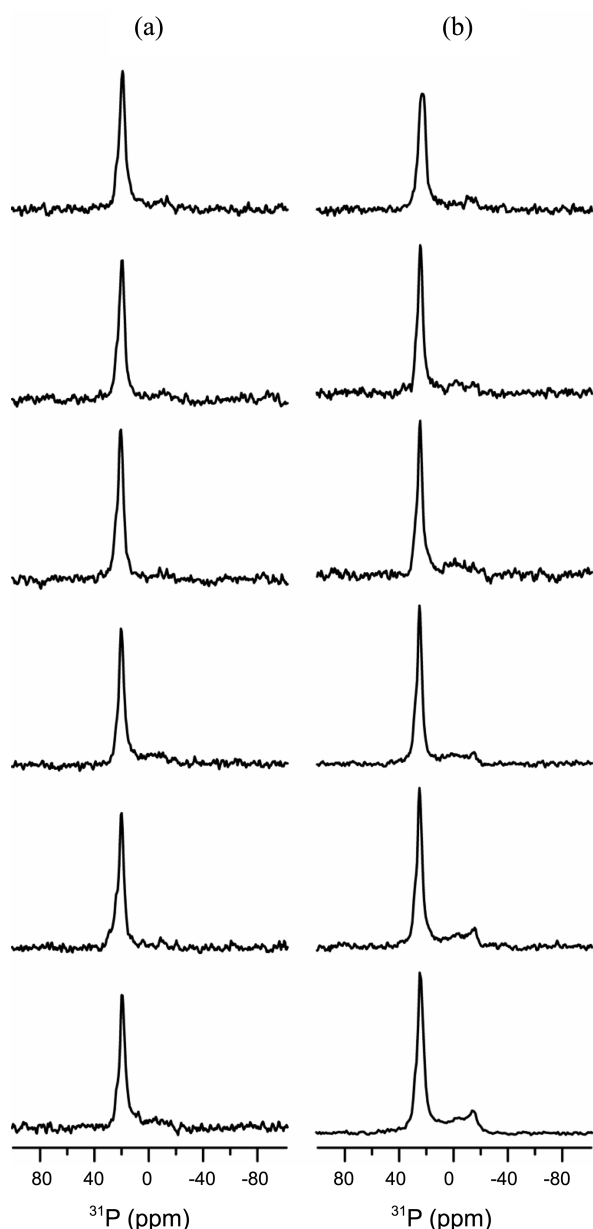


**Figure 4.**  $^{31}\text{P}$  SSNMR spectral changes of POPC/cholesterol multi-bilayers by PG-1. (a) 20, 40 minutes and 5, 17, 40, 66 hours (from top to bottom) when hydrated at 95% humidity. (b) 20, 70 minutes, and 2, 6.5, 47, 316 hours (from top to bottom) after fully hydrating the sample by adding water.

95% relative humidity. 35% was disrupted when fully hydrated (Fig. 4). The effect of cholesterol on the peptide activity was similar at both hydration levels. Bilayer disruption was reduced by 2.5 times in the presence of cholesterol. P/L ratios of the peptide-lipid aggregates at 95% relative humidity and at full hydration were 1:2 and 1:7, respectively, assuming that all the peptide molecules aggregated with the lipid.

In contrast to the isotropic phase of the PG-1 and POPC mixture, the peptide-lipid aggregates in the POPC/cholesterol bilayers showed random powder patterns even at full hydration. Assuming that the aggregates were spherical, e.g.

vesicles, the aggregates that contained cholesterol had over 30 times the radius of those that did not contain cholesterol, when the radius was calculated from their rotational diffusion coefficients obtained by fitting the  $^{31}\text{P}$  SSNMR spectra with a rotational diffusion model.

These results are consistent with the cholesterol-containing lipid membrane being much more stable against attack by antimicrobial peptides. Tight lipid packing in POPC biomembranes is not possible due to a *cis* double bond in the molecule, which lead to them having bent tails that allow the lipid molecules to move easily in the lateral plane of the membrane. Cholesterol, however, immobilizes the hydrocarbon tails of POPC molecules, particularly their first few methylene groups, increasing the rigidity of the membrane surface.<sup>44</sup> More rigid membranes require greater peptide accumulation on their surfaces before breaking. Geometrically, cholesterol makes a membrane curvature more negative.<sup>45</sup> When the bilayer phase of a lipid membrane is disrupted by a peptide inducing positive curvature, such as PG-1,<sup>45</sup> it generally has a positive curvature. Therefore cholesterol-containing lipid membranes require higher peptide concentrations on their surfaces before breaking because of their decreased curvature. Their lower curvature led to the aggregates with cholesterol being larger than those without, assuming spherical aggregates. The observed increases of PG-1 critical concentration and aggregate size were consistent with cholesterol effects on the curvature of lipid bilayers.

Disruption of the cholesterol-containing POPC bilayers was much slower than of the pure POPC bilayers, though it could not be exactly quantified. The slower rate of disruption is consistent with the larger peptide-cholesterol-lipid aggregates decreasing the diffusion rate of the free peptides. However, the stabilizing effects of the cholesterol molecules on the membrane surfaces did not greatly affect the uniaxial rotational motion of lipid molecules, which was confirmed by the unchanged width of  $^{31}\text{P}$  SSNMR spectra (Fig. 3).

**Comparison of Two Experimental Methods.** In the previous paper authors investigated the pore structure induced by the PG-1 peptide and obtained the lateral diffusion coefficient of the lipid molecules composing the pore.<sup>46</sup> The sample was prepared by mixing the peptides and the lipids simultaneously and homogeneously.  $^{31}\text{P}$  SSNMR spectra were recorded of POPC lipids both in homogeneously mixed peptide-lipid phases and in heterogeneously mixed samples that has reached equilibrium (Fig. 5). All the POPC molecules in the homogeneously mixed sample without cholesterol were disrupted by PG-1, as shown by the single peak at 0 ppm (Fig. 5(c)). However, a portion of the lipid molecules remained as bilayers in the heterogeneously mixed samples, they showed a peak at 28 ppm (Fig. 5(a)). Their broader peak at around 0 ppm suggests that their disrupted peptides-lipid aggregations were generally larger and more diversely sized. Figure 5(d) shows that a large portion of POPC lipid molecules were disrupted by PG-1 in the homogeneously mixed sample despite the presence of cholesterol. However, a small portion of the POPC/chole-

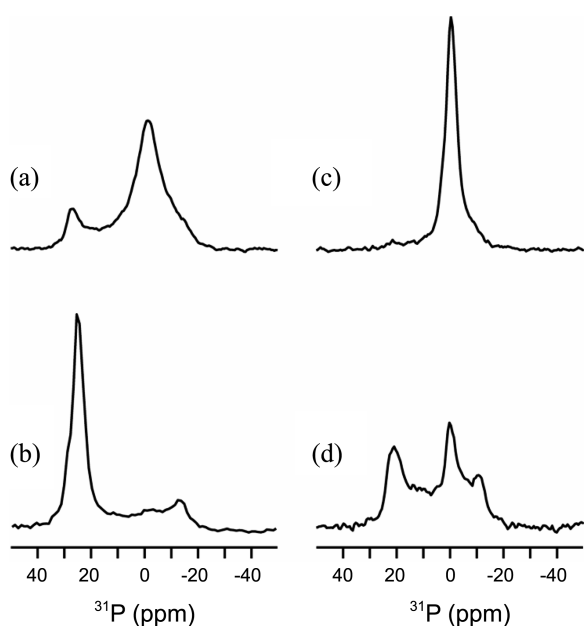


**Figure 5.** Comparison of  $^{31}\text{P}$  SSNMR spectra of POPC when mixed with PG-1. (a) and (b) are the heterogeneously mixed samples in the absence and the presence of cholesterol, respectively. (c) and (d) are the homogeneously mixed samples in the absence and the presence of cholesterol, respectively.

sterol bilayers were disrupted by PG-1 in the heterogeneously mixed sample (Fig. 5(b)). All samples were made at full hydration using the same concentrations of peptide and lipid on the glass plates.

Heterogeneously mixed sampling better represented the antimicrobial peptide invasion of biomembranes than homogeneously mixed sampling. The disruption by AMP of natural cell membranes begins with its binding to the bilayered membrane surface. An intermediate state must form before the final disrupted peptide-membrane phase, which acts as an energy barrier to disruption. The heterogeneously mixed samples underwent peptide-binding and therefore encountered this energy barrier, while the homogeneously mixed samples method did not. This difference led to different final states in the peptide-lipid mixtures. Heterogeneous mixing showed a critical concentration of peptide similar to that observed physiologically. However assessing that of the homogeneously mixed samples was difficult by performing a single experiment. These results suggest that peptide binding on membrane surfaces is important in the overall mechanism of lipid bilayer disruption by AMP. The effects of peptide-binding will be investigated in greater detail by further studies of various lipids using AMP at various concentrations.

### Conclusions

The effects of hydration and cholesterol on the action of antimicrobial peptide on lipid bilayers were investigated by  $^{31}\text{P}$  SSNMR spectroscopy of mechanically aligned bilayers. The relative reaction rates and the critical concentrations of

PG-1 under different hydration conditions were measured for its action on lipid membranes. They could not be assessed using homogeneously mixed peptide-lipid samples. The action of the antimicrobial peptide PG-1 was slower and more limited when samples were hydrated at 95% relative humidity. The presence of cholesterol also hindered its activity. The effects of hydration were unaffected by the presence of cholesterol: disruption consistently increased by 2.5 times upon full hydration. Heterogeneously mixed samples allowed more quantitative assessment of the effects of hydration and cholesterol than homogeneously mixed samples. They also allowed direct measurement of the effects of hydration at various hydration levels simply by adding different amounts of water to dried bilayer samples. While this novel methodology can yet be improved theoretically and experimentally, it has demonstrated strong potential to aid the study of the disruption mechanisms of various antimicrobial peptides.

**Acknowledgments.** This work was supported by the Basic Science Research Program through the National Research Foundation of Korea (NRF) funded by the Ministry of Education, Science and Technology (2010-0011558).

**Supplementary Materials.** Supplementary figure S1 is available at the bkcs website.

### References

- Hallock, K. J.; Lee, D. K.; Ramamoorthy, A. *Biophys. J.* **2003**, *84*, 3052.
- Hwang, P. M.; Vogel, H. J. *Biochem. Cell Biol.* **1998**, *76*, 235.
- Zaslloff, M. *Proc. Natl. Acad. Sci. U. S. A.* **1987**, *84*, 5449.
- Buffy, J. J.; Waring, A. J.; Hong, M. *J. Am. Chem. Soc.* **2005**, *127*, 4477.
- Yeaman, M. R.; Yount, N. Y. *Pharmacol. Rev.* **2003**, *55*, 27.
- Moraes, C. M.; Bechinger, B. *Magn. Reson. Chem.* **2004**, *42*, 155.
- Mani, R.; Waring, A. J.; Lehrer, R. I.; Hong, M. *Biochim. Biophys. Acta, Biomembr.* **2005**, *1716*, 11.
- Mani, R.; Buffy, J. J.; Waring, A. J.; Lehrer, R. I.; Hong, M. *Biochemistry* **2004**, *43*, 13839.
- Yamaguchi, S.; Hong, T.; Waring, A.; Lehrer, R. I.; Hong, M. *Biochemistry* **2002**, *41*, 9852.
- Marasinghe, P. A. B.; Buffy, J. J.; Schmidt-Rohr, K.; Hong, M. *J. Phys. Chem. B* **2005**, *109*, 22036.
- Pokorny, A.; Almeida, P. F. F. *Biochemistry* **2005**, *44*, 9538.
- Matsuzaki, K. *Biochim. Biophys. Acta, Rev. Biomembr.* **1998**, *1376*, 391.
- Matsuzaki, K.; Murase, O.; Fujii, N.; Miyajima, K. *Biochemistry* **1995**, *34*, 6521.
- Matsuzaki, K.; Sugishita, K.-i.; Ishibe, N.; Ueha, M.; Nakata, S.; Miyajima, K.; Epand, R. M. *Biochemistry* **1998**, *37*, 11856.
- Herasimenka, Y.; Benincasa, M.; Mattiuzzo, M.; Cescutti, P.; Gennaro, R.; Rizzo, R. *Peptides* **2005**, *26*, 1127.
- Richard, J.-A.; Kelly, I.; Marion, D.; Pezolet, M.; Auger, M. *Biophys. J.* **2002**, *83*, 2074.
- Ludtke, S. J.; He, K.; Heller, W. T.; Harroun, T. A.; Yang, L.; Huang, H. W. *Biochemistry* **1996**, *35*, 13723.
- Matsuzaki, K.; Murase, O.; Tokuda, H.; Funakoshi, S.; Fujii, N.; Miyajima, K. *Biochemistry* **1994**, *33*, 3342.
- Matsuzaki, K.; Murase, O.; Miyajima, K. *Biochemistry* **1995**, *34*, 12553.

20. Valcarcel, C. A.; Dalla Serra, M.; Potrich, C.; Bernhart, I.; Tejuca, M.; Martinez, D.; Pazos, F.; Lanio, M. E.; Menestrina, G. *Biophys. J.* **2001**, 80, 2761.
  21. Bechinger, B. *Biochim. Biophys. Acta, Biomembr.* **2005**, 1712, 101.
  22. Mani, R.; Tang, M.; Wu, X.; Buffy, J. J.; Waring, A. J.; Sherman, M. A.; Hong, M. *Biochemistry* **2006**, 45, 8341.
  23. Mecke, A.; Lee, D.-K.; Ramamoorthy, A.; Orr, B. G.; Holl, M. M. *Biophys. J.* **2005**, 89, 4043.
  24. Jang, H.; Ma, B.; Woolf Thomas, B.; Nussinov, R. *Biophys. J.* **2006**, 91, 2848.
  25. Heller, W. T.; Waring, A. J.; Lehrer, R. I.; Harroun, T. A.; Weiss, T. M.; Yang, L.; Huang, H. W. *Biochemistry* **2000**, 39, 139.
  26. Shai, Y. *Biochim. Biophys. Acta, Biomembr.* **1999**, 1462, 55.
  27. Wu, M.; Maier, E.; Benz, R.; Hancock, R. E. W. *Biochemistry* **1999**, 38, 7235.
  28. Matsuzaki, K. *Biochim. Biophys. Acta, Biomembr.* **1999**, 1462, 1.
  29. Yang, L.; Harroun, T. A.; Weiss, T. M.; Ding, L.; Huang, H. W. *Biophys. J.* **2001**, 81, 1475.
  30. Huang, H. W. *Biochemistry* **2000**, 39, 8347.
  31. Yang, L.; Weiss, T. M.; Lehrer, R. I.; Huang, H. W. *Biophys. J.* **2000**, 79, 2002.
  32. Kokryakov, V. N.; Harwig, S. S.; Panyutich, E. A.; Shevchenko, A. A.; Aleshina, G. M.; Shamova, O. V.; Korneva, H. A.; Lehrer, R. I. *FEBS Lett.* **1993**, 327, 231.
  33. Hallock, K. J.; Lee, D.-K.; Omnaas, J.; Mosberg, H. I.; Ramamoorthy, A. *Biophys. J.* **2002**, 83, 1004.
  34. Washburn, E. W.; West, C. J.; Hull, C. *International Critical Tables of Numerical Data, Physics, Chemistry, and Technology*; McGraw-Hill: New York, 1926.
  35. Oren, Z.; Shai, Y. *Biopolymers* **1998**, 47, 451.
  36. Zasloff, M. *Nature* **2002**, 415, 389.
  37. Domene, C.; Bond, P. J.; Deol, S. S.; Sansom, M. S. P. *J. Am. Chem. Soc.* **2003**, 125, 14966.
  38. Manna, M.; Mukhopadhyay, C. *Langmuir: The ACS Journal of Surfaces and Colloids* **2009**, 25, 12235.
  39. Norbert Kučerka, S. T.-N.; John, F. N. *J. Membrane Biol.* **2005**, 208, 193.
  40. Ludtke, S. J.; He, K.; Wu, Y.; Huang, H. W. *Biochim. Biophys. Acta, Biomembr.* **1994**, 1190, 181.
  41. Vogel, M.; Munster, C.; Fenzl, W.; Salditt, T. *Phys Rev Lett* **2000**, 84, 390.
  42. Chen, F. Y.; Hung, W. C. *Chinese Journal of Physics* **1996**, 34, 1363.
  43. Buffy, J. J.; McCormick, M. J.; Wi, S.; Waring, A.; Lehrer, R. I.; Hong, M. *Biochemistry* **2004**, 43, 9800.
  44. O'Brien, J. S. *Science* **1965**, 147, 1099.
  45. Mani, R.; Cady, S. D.; Tang, M.; Waring, A. J.; Lehrer, R. I.; Hong, M. *Proc. Natl. Acad. Sci. U. S. A.* **2006**, 103, 16242.
  46. Wi, S.; Kim, C. *J Phys Chem B* **2008**, 112, 11402.
-